

# HIGH-CYCLE FATIGUE CRACK PATHS IN SPECIMENS HAVING DIFFERENT STRESS CONCENTRATION FEATURES

G. Meneghetti<sup>1</sup>, L. Susmel<sup>2</sup>, R. Tovo<sup>2</sup>

<sup>1</sup>Department of Mechanical Engineering - University of Padova  
Via Venezia, 1 - 35131 Padova (Italy)

<sup>2</sup>Department of Engineering - University of Ferrara  
Via Saragat, 1 - 44100 Ferrara (Italy)

E-mail: giovanni.meneghetti@unipd.it, lsusmel@ing.unife.it, rtovo@ing.unife.it

## Abstract

This paper summarises on an attempt to study the high-cycle fatigue cracking behaviour in specimens of low carbon steel weakened by U-notches. The considered  $K_t$  values, calculated with respect to the gross area, ranged from 3.8 up to about 25. The specimens were tested under uniaxial fatigue loading with a load ratio equal to 0.1. The observed cracking behaviour proved the fact that a Stage 1-like process can always be assumed to be representative of the crack initiation phenomenon, independently of the  $K_t$  value. This result seems to support the idea that crack initiation is Mode II governed independently of the stress concentration feature weakening the material. This experimental evidence is very interesting, because it could represent a sound framework on which the extension of the critical plane approaches to multiaxial notch fatigue situations could be based.

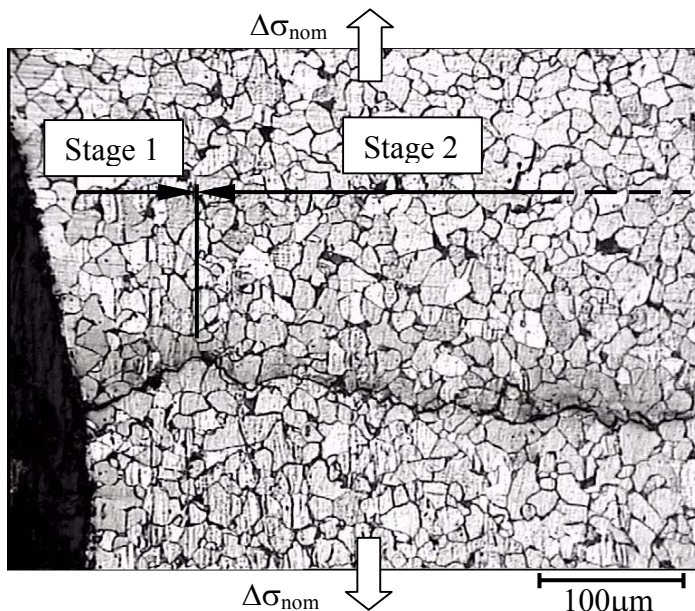


FIGURE 1. Crack path in a blunt notched specimen ( $K_{tg}=5.7$ ). The crack was generated in the medium cycle fatigue regime ( $N_f=480148$  cycles to failure).

(or by the first micro-structural barrier) [2, 3]. On the contrary, when specimens are weakened by sharp notches, the non-propagating crack length is much larger, that is, it is of the order of the material characteristic length,  $L$  [4].

## Introduction

Uniaxial fatigue failures in plain specimens are characterised by crack paths showing two different stages (Fig. 1) [1]: Stage 1 is mainly mode II dominated and its length covers few grains; on the contrary, Stage 2 is mainly mode I governed. To be precise, when Stage 1 is about to be exhausted, cracks tend to orient themselves in order to experience the maximum principal stress range.

The fatigue limit condition is given by the formation of a non-propagating crack emanated from specimen's weakest point. In plain specimens, the propagation of this kind of cracks is arrested by the first grain boundary

It is important to highlight here that estimating the fatigue limit of un-cracked bodies is mainly a short crack problem. In this situation, the material cracking behaviour principally depends on the real material morphology close to the apex of the stress concentrator: linear elastic stresses calculated at the notch tip are not meaningful and the physical phenomena taking place in the fatigue process zone can correctly be described just by considering grain plasticity [5]. Only when cracks become long (that is, when their length is larger than about  $10L$ ), linear elastic stresses are representative of the crack propagation phenomenon: this is the only ambit in which the LEFM theory can correctly be used.

In this study, specimens having different stress concentration features were tested in the high-cycle fatigue regime in order to study the early stage of crack growth in the presence of notches. The generated failures were then used to create a bridging between the engineering diagram proposed by Smith and Miller [6] and the observed material cracking behaviour. Finally, Susmel's fatigue damage model [7] was applied to show that just one formulation can be employed to predict notched fatigue limits independently of the  $K_t$  value.

## Experimental details and results

The tested specimens were made of C10, a commercial low carbon steel, having the following mechanical properties: ultimate tensile stress  $\sigma_{UTS}=412$  MPa; yield stress  $\sigma_Y=263$  MPa, average grain size  $0.18\mu\text{m}$ , plain fatigue limit  $\Delta\sigma_0=360$  MPa ( $R=0.1$ ), threshold value of the stress intensity factor  $\Delta K_{th}=5.6$  MPa $\cdot\text{m}^{1/2}$  ( $R=0.1$ ) and, finally, the material characteristic length [8] was equal to:

$$L = \frac{1}{\pi} \left( \frac{\Delta K_{th}}{\Delta\sigma_0} \right)^2 = 0.08 \text{ mm} \quad (1)$$

The geometries of the tested specimens as well as the values of the stress concentration factors, referred to the gross area, are reported in Fig. 2. These specimens were tested in load control, under a load ratio,  $R$ , equal to 0.1 and with a frequency ranging from 30 up to 35 Hz. Fatigue failure was defined by 10% stiffness drop, which resulted in cracks, emanated from the tip of one of the two notches, having a length of about 5mm.

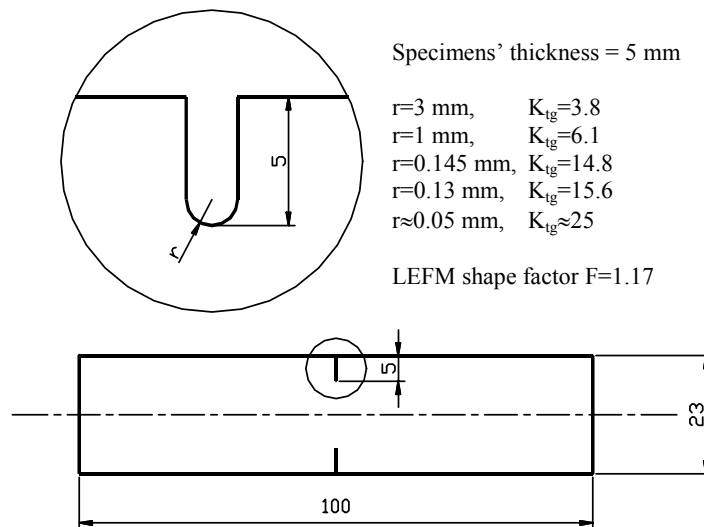


FIGURE 2. Geometries of the tested specimens.

In the present study only failures occurred in the high-cycle fatigue regime (that is, ranging from  $10^6$  up to  $3.5 \cdot 10^6$  cycles to failure) were considered. The observed cracks were assumed to be representative of the material cracking behaviour in a fatigue region close to the nominal notched fatigue limit. The generated results are summarised in Smith and Miller's diagram reported in Fig. 4.

## Material cracking behaviour

In order to study the material cracking behaviour, the cracked specimens were polished up to a mirror-like finish. Subsequently, specimens' surfaces were etched to show the grain distribution. Fatigue crack paths were then inspected by using a LEICA MEF4M microscope with a JVC TK-C1380 digital camera. Pictures and measurements were managed using the A4i Docu software.

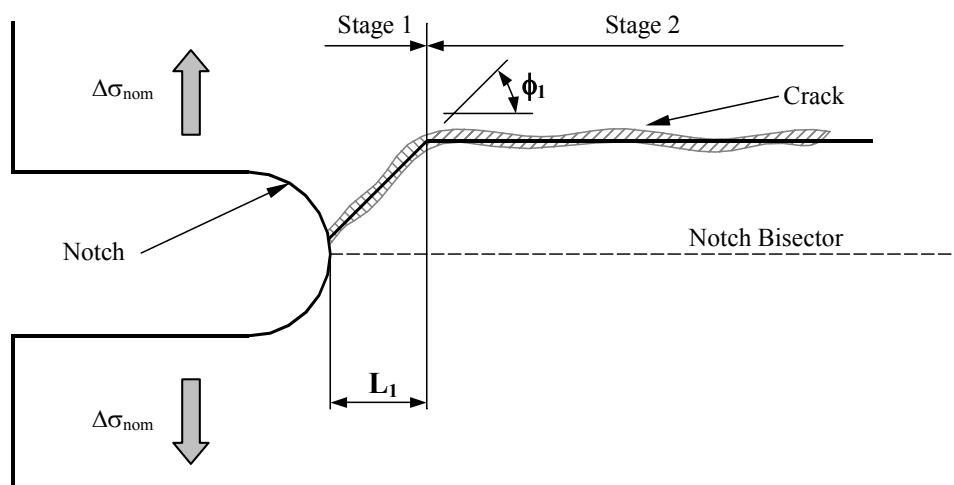


FIGURE 3. Length and orientation of Stage 1.

Initially, it is important to highlight that the tested specimens were definitively thick. Hence, it is possible to presume that, in some situations, crack initiations occurred at the centre of the specimen thickness [9]. In any case, the direct inspection of the crack surfaces showed that the elliptical crack fronts were characterised by a negligible curvature. For this reason, the orientations of the cracks measured on the two surfaces of every specimen (even though they were slightly different) were assumed to give representative information on the orientation of the plane where Stage 1 took place.

Figure 3 summarises the schematisation adopted to define length and orientation of Stage 1 by the length  $L_1$  and the angle  $\phi_1$ , respectively.

In Fig. 4, the experimental results used to study the material cracking behaviour in the presence of different  $K_{tg}$  values are summarised in a Smith and Miller's diagram. We plotted these data in such a diagram because the results reported there were generated applying nominal stress ranges close to the corresponding notched fatigue limits: for the stress range values plotted in the diagram, at least two run-outs for every considered  $K_{tg}$  value have always been obtained. Moreover, In Fig. 4 it has been reported some pictures showing the orientation of the Stage 1 plane in specimens having different  $K_{tg}$  values.

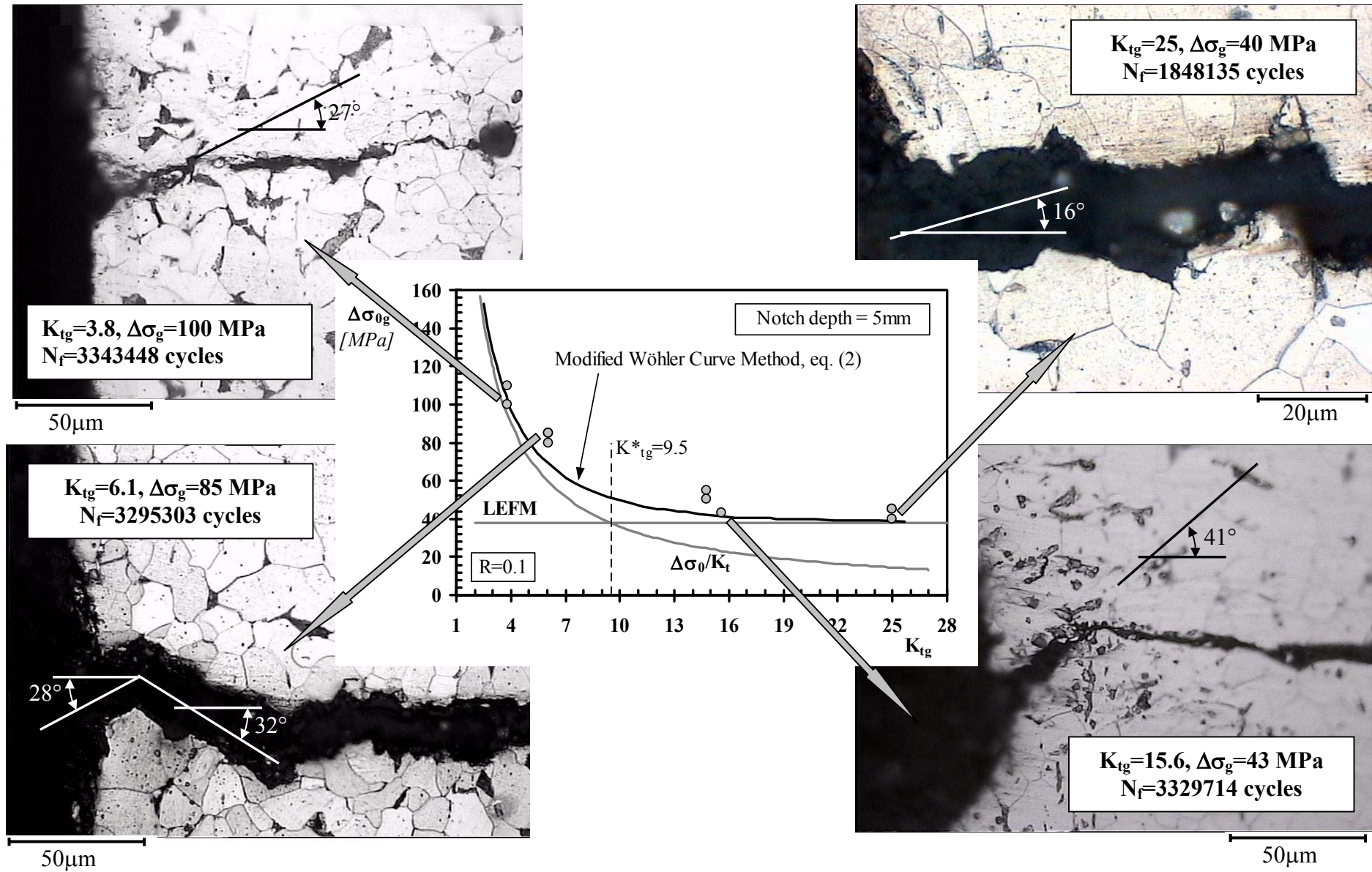


FIGURE 4. Early stage of the crack growth in specimens characterised by different  $K_{tg}$  values and Smith and Miller's diagram.

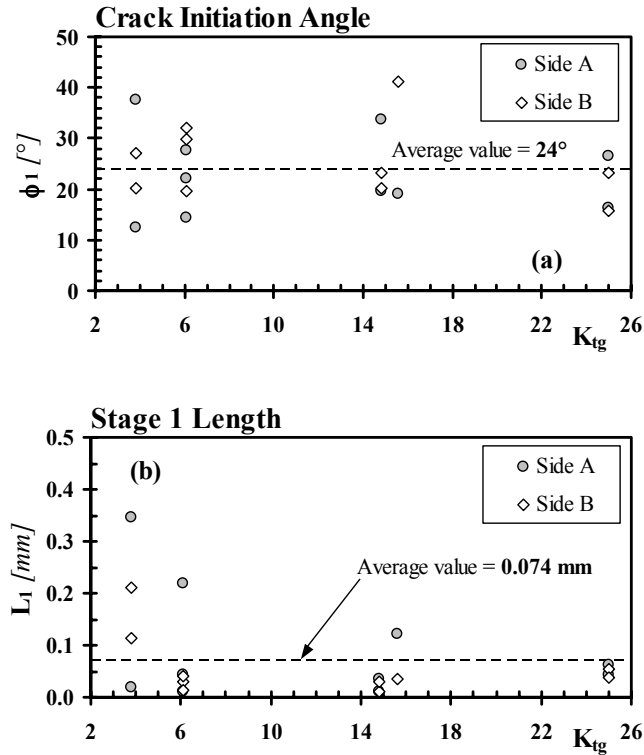


FIGURE 5. Orientation (a) and length (b) of Stage 1 for different values of  $K_{tg}$ .

agreement with the classical Kitagawa-Takahashi diagram [10]: within a length interval of about  $L$  meso-cracks tended to orient themselves to experience the maximum principal stress range. Only when the length of the observed cracks was much larger than  $L$ , they became long-cracks following the behaviour predicted by the LFM theory.

## The fatigue damage model

The generated experimental results seem to strongly support the idea that crack initiation is always mode II dominated, and it holds true independently of the  $K_{tg}$  value. As shortly said above, crack initiation is a short crack problem and, strictly speaking, it could rigorously be described just by considering both the real material morphology in the vicinity of crack initiation site and the elasto-plastic material behaviour. Unfortunately, such an approach, even though it is attractive from a scientific point of view, it would be too cumbersome to be applied in an industrial reality.

To overcome this problem, recently, Susmel proposed a new fatigue damage model suitable for predicting the high-cycle fatigue strength of notched components subjected to any kind of fatigue loading [7]. This approach is based on the following assumptions (Fig. 6):

- 1) Independently of the geometrical feature, initiation and initial growth of micro/meso-cracks are mixed-mode governed. This process can be assumed to be similar to the classical Stage 1 taking place in smooth components;
- 2) In fatigue limit conditions, all the cracking processes are confined within the structural volume;
- 3) For a given material, the size of the structural volume is constant and directly related to the characteristic material length constant,  $L$  (determined under  $R=-1$ );

These pictures highlight that, independently of the  $K_t$  value, the early stage of the crack propagation was, in general, mainly mode II dominated. To be precise, Stage 1 planes were never parallel to the notch bisector. This statement is strongly supported by Fig. 5a. In this diagram the two crack initiation angles measured on the two surfaces of every specimen (Side A and B in Fig. 5) are plotted against  $K_{tg}$ . This diagram makes it evident that, independently of the  $K_{tg}$  value,  $\phi_1$  ranged from  $10^\circ$  up  $40^\circ$  and the average value was equal to  $24^\circ$ .

The Stage 1 lengths measured on the two surfaces of the tested specimens are summarised in Fig. 5b. The  $L_1$  vs.  $K_{tg}$  diagram shows that Stage 1 lengths tended to decrease as the  $K_{tg}$  value increased. The average value was equal to  $0.074$  mm, which was very close to the material characteristic length,  $L$ , of the tested material. This result is in

- 4) In fatigue limit conditions, some micro/meso-cracks are always present within the structural volume;
- 5) In fatigue limit conditions, the linear-elastic stress state at the centre of the structural volume is representative of the entire stress field damaging the fatigue process zone;
- 6) The fatigue damage due to an ideal Stage 1-like process reaches its maximum value on a critical plane defined as the one experiencing the maximum shear stress amplitude,  $\tau_a$ . Moreover, the amount of fatigue damage also depends on the maximum stress normal to the critical plane,  $\sigma_{n,max}$ .

According to the Modified Wöhler Curve Method method, mechanical components are in fatigue limit condition when the following condition is assured:

$$\tau_a + \left( \tau_0 - \frac{\sigma_0}{2} \right) \cdot \frac{\sigma_{n,max}}{\tau_a} \leq \tau_0 \quad (2)$$

where  $\sigma_0$  and  $\tau_0$  are the fully-reversed plain uniaxial and torsional fatigue limit, respectively.

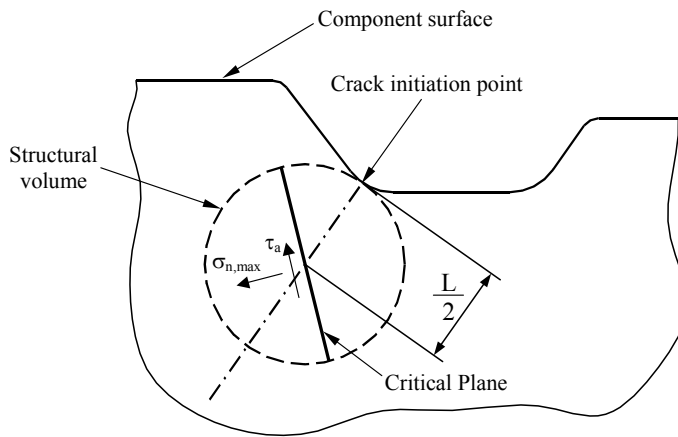


FIGURE 6. Structural Volume and Critical Plane definition according to Susmel's fatigue damage model.

The maximum shear stress amplitude,  $\tau_a$ , and the maximum normal stress,  $\sigma_{n,max}$ , relative to the critical plane must be determined considering the stress state calculated at that point which is positioned along a straight line emanating from the assumed crack initiation site and perpendicular to the component surface (Fig. 6).

This method was seen to be a sound tool suitable for predicting the high-cycle fatigue strength in the presence of any kind of geometrical feature and under any kind of fatigue loading [7].

The experimental results discussed in the present paper seem to strongly support the validity of the first assumption on which this method is based: shear stress plays a fundamental role in the early stage of the crack propagation phenomenon. For this reason, this experimental evidence may prove the fact that our approach is soundly connected to the physical mechanisms damaging metal materials under cyclic loading.

TABLE 1. Material Fatigue Properties [11] used to plot the diagrams reported in Fig. 7 (Torsional fatigue limits estimated by using Von Mises' formula).

Material	R	$\sigma_0$ / MPa	$\tau_0$ / MPa	$\Delta K_{th}$ / MPa m <sup>1/2</sup>	L / mm
SAE 1045	-1	303	175	9.0	0.07
	0	224		6.9	
2024-T351	-1	124	72	4.4	0.10
	0	86		4.0	
SM41B	-1	163	94	12.4	0.46
	0	137		8.4	
	0.4	122		6.4	

It is important to highlight here that, even though our method is linked to the essence of the studied phenomenon, it cannot be used to predict the real crack initiation path. In fact, the use of linear-elastic stresses makes our method accurate enough to be used for the engineering estimation of the fatigue limit. Nevertheless, it is evident that linear-elastic stress fields are not sensitive neither to the real material morphology nor to the grain plasticity, so that, our method can supply just approximate information on the real crack paths.

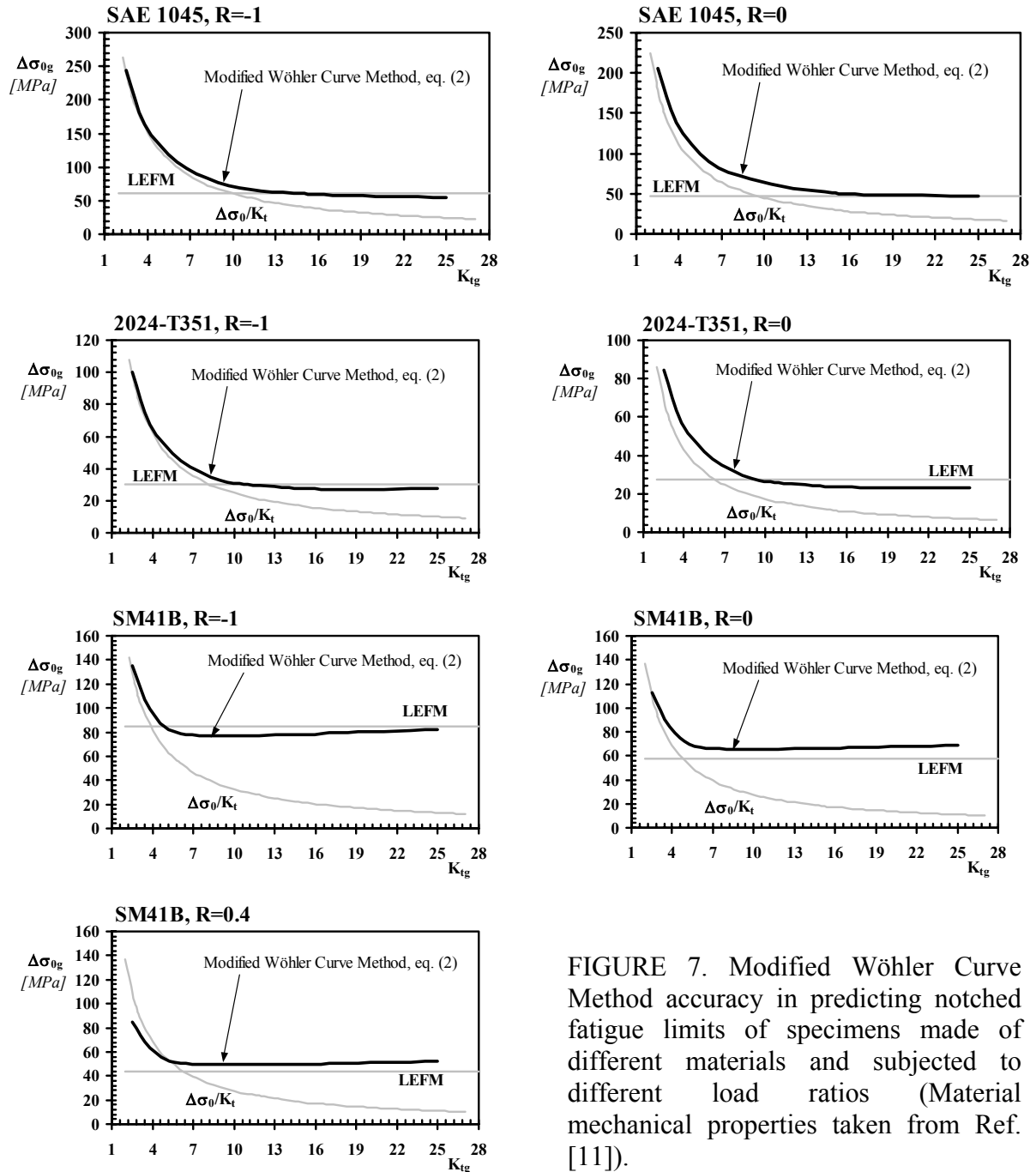


FIGURE 7. Modified Wöhler Curve Method accuracy in predicting notched fatigue limits of specimens made of different materials and subjected to different load ratios (Material mechanical properties taken from Ref. [11]).

To prove what we stated in the previous paragraph, Eq. (2) has been used to estimate the high cycle fatigue strength of the tested specimens. The application of our method requires the fully-reversed uniaxial and torsional fatigue limit. Unfortunately, the only available mechanical properties for the tested material were the plain fatigue limit determined under  $R=0.1$  and the ultimate tensile stress. The fully-reversed uniaxial fatigue limit was estimated

by using Goodman's hypothesis, obtaining:  $\sigma_{0, R=-1}=386$  MPa, whereas, the fully-reversed torsional fatigue limit was calculated according to Von Mises' hypothesis:  $\tau_{0, R=-1}=223$  MPa.

The curve plotted on the Smith and Miller diagram reported in Fig. 3 shows that our method is capable of correctly describing the entire field of interest, satisfactorily interpolating the two asymptotic curves given by the stress-life method and by the LEFM theory, respectively. The problem of this interpolating curve is that our method was applied using the characteristic length value calculated under a load ratio,  $R$ , equal to 0.1, whereas its rigorous application requires the use of a  $L$  length determined under  $R=-1$ . Apart from that, the accuracy showed by eq. (2) can be considered to be representative of our method's reliability, mainly because both calibration fatigue limits were estimated.

In any case, to better check the validity of our method, a further validation was done again considering the geometries sketched in Fig. 2, but assuming that the specimens were made of different materials. The mechanical properties of these materials, summarised in Tab. 1, were taken from the literature [11]. Figure 7 confirms the fact that our method is capable of interpolating the entire field of interest in Smith and Miller's diagram, even if the fully-reversed torsional fatigue limit was estimated using Von Mises' formula. Moreover, observing that our approach was calibrated just using mechanical properties generated under  $R=-1$ , the diagrams in Fig. 7 confirm that our method is capable of satisfactorily accounting for also the mean stress effect.

## Conclusions

The experimental tests carried out proved the fact that initiation and initial growth of cracks emanating from the tip of notches are always mixed-mode governed, and it holds true independently of the  $K_t$  value. This experimental evidence allowed us to use the Modified Wöhler Curve Method to predict the notch fatigue limit of the tested specimens: our method was seen to be a sound tool to assess notched components in situation of practical interest.

## References

1. Miller, K. J., *Fatigue Fract. Engng. Mater. Struct.*, vol. **16**, 931-939, 1993.
2. Usami, S., In: *Current Japanese Materials Research*, Vol. I, Ed. by T. Tanaka et al., 119-147, 1998.
3. Akiniwa, Y., et al., *Fatigue Fract. Engng. Mater. Struct.*, vol. **24**, 817-829, 2001.
4. Taylor, D., *Fatigue Fract. Engng. Mater. Struct.*, vol. **24**, 215-224, 2001.
5. Tomkins, B., *Philosophical Magazine*, 1041-1066, 1968.
6. Smith, R. A., Miller, K. J., *Int. J. Mech. Sci.*, vol. **20**, 201-206, 1978.
7. Susmel, L., *Fatigue Fract. Engng. Mater. Struct.*, vol. **27**, 391-411, 2004.
8. Taylor, D., *Int. J. Fatigue*, vol. **21**, 413-420, 1999.
9. Lukas, P., et al., *Fatigue Fract. Engng. Mater. Struct.* **9**, 195-204, 1986.
10. Kitagawa, H., Takahashi, S. In *Proc. of 2<sup>nd</sup> Int. Conference on Mechanical Behaviour of Materials*, Boston, 1976, 627-631.
11. Atzori, B., Lazzarin, P., Meneghetti G., *Fatigue Fract. Engng. Mater. Struct.*, vol. **26**, 257-268, 2003.